Electronic Supplementary information (ESI)

for

Solution and solid-state interactions in a supramolecular ruthenium photosensitizer–polyoxometalate aggregate

by

Kirsten Heussner[a], Katrin Peuntinger[b], Nils Rockstroh[a], Leanne Nye[c], Ivana Ivanovic-Burmazovic[c], Sven Rau[a]* and Carsten Streb[a]*

[a]Institute of Inorganic Chemistry II; [b]Institute of Physical Chemistry I, [c]Institute of Bioinorganic Chemistry, Department of Chemistry and Pharmacy, Friedrich-Alexander-University Erlangen-Nuremberg, Egerlandstr. 1, 91058 Erlangen, Germany.
*Email: carsten.streb@chemie.uni-erlangen.de; sven.rau@chemie.uni-erlangen.de

1. Instrumentation

X-ray diffraction: Single-crystal X-ray diffraction studies were performed on a Nonius Kappa CCD Single-crystal X-ray diffractometer equipped with a graphite monochromator using MoK_α radiation (wavelength λ(MoK_α) = 0.71073 Å).

NMR spectroscopy: ^{1}H- and ^{13}C-NMR spectroscopy was performed on a JEOL EX 400 NMR spectrometer using deuterated solvents as internal standards.

Steady state UV-Vis absorption spectroscopy: Steady state absorption spectra were obtained using a Varian Cary 50 spectrophotometer or a Perkin Elmer Lambda2 UV-Vis two-beam spectrophotometer using a slit width of 2 nm and a scan rate of 480 nm/min. All spectra were recorded using a quartz glass cuvette of 10x10 mm.

Emission spectroscopy: Emission spectroscopy was performed on a r using an excitation wavelength of 497 nm.

Steady state emission spectroscopy: Steady state emission spectra were recorded using a JASCO FP-6300 Fluorescence spectrophotometer or a Horiba Jobin Yvon FluoroMax-3 spectrometer using an excitation wavelength of 497 nm, slit width of 5 nm for excitation and emission and an integration time of 0.5 s. The studies were performed in a 10x10 mm quartz glass cuvette.

FT-IR spectroscopy: FT-IR spectroscopy was performed on a Shimadzu FT-IR-8400S spectrometer. Samples were prepared as KBr pellets. Signals are given as wavenumbers in cm^{-1} using the following abbreviations: vs = very strong, s = strong, m = medium, w = weak and b = broad.

Elemental analysis: Elemental analysis was performed on a Euro Vector Euro EA 3000 Elemental Analyzer.

Mass spectrometry: ESI-MS spectra were recorded on a Bruker Daltonics maXis ultra high resolution ESI-Time-Of-Flight MS. Spectra were obtained in negative-ion mode. Peaks were identified using simulated isotopic patterns created within the Bruker DataAnalysis software.

General remarks: All chemicals were purchased from Sigma Aldrich or ACROS and were of reagent grade. Solvents used were of p.a. grad unless stated otherwise. Chemicals and solvents were used without further purification unless stated otherwise. Compound **1** was prepared as described in the literature.[S1] Compound **2** was prepared according to the literature by replacing triethylammonium counterions with tetra-*n*-butylammonium (TBA) counterions.[S2] Product purity was confirmed using elemental analysis, ^{1}H-NMR-, UV-Vis- and FT-IR spectroscopy.

2. Synthetic section

2.1. Synthesis of compound **3**: $[Ru(tbbpy)_2(biH_2)]_2[Mo_8O_{26}]$ x *ca.* 5 DMSO:
$[(tbbpy)_2Ru(biH_2)(PF_6)_2]$ (104 mg, 96.2 µmol) was dissolved in 15 ml DMSO. A solution of $TBA_4[Mo_8O_{26}]$ (414 mg, 192.7 µmol) in 15 ml DMSO was added and the mixture was stirred overnight. Diffraction quality crystals were obtained by slow diffusion of ethyl acetate into the clear reaction mixture. Deep red block crystals were collected after approximately four weeks. The crystals were washed with methanol and dried under vacuum. Yield: 34 mg (12.1 µmol, 25.1 % based on Ru). Elemental analysis (dried material) for $C_{84}H_{108}Mo_8N_{16}O_{26}Ru_2$ in wt.-% (calcd.): C 36.17 (36.99), H 3.80 (3.99), N 7.84 (8.22). Characteristic IR bands (in cm^{-1}): 3482 (s), 2972 (s), 1619 (s), 1543 (m), 1482 (m), 1415 (m), 1385 (s), 1254 (w), 1133 (w), 1033 (w), 949 (s), 919 (s), 852 (m), 808 (m), 719 (m), 668 (s).

3. Crystallographic section

Single-Crystal Structure Determination: Suitable single crystals of the respective compound were grown and mounted onto the end of a thin glass fiber using Fomblin oil. X-ray diffraction intensity data were measured at 150 K on a Nonius Kappa CCD diffractometer [λ(Mo-K_α) = 0.71073 Å] equipped with a graphite monochromator. Structure solution and refinement was carried out using the SHELX-97 package[S3] *via* WinGX.[S4] Corrections for incident and diffracted beam absorption effects were applied using empirical[S5] or numerical methods.[S6] Structures were solved by a combination of direct methods and difference Fourier syntheses and refined against F^2 by the full-matrix least-squares technique. Diffuse solvent correction was carried out using the SQUEEZE function in Platon.[S7] The two hydrogen atoms located on the biH_2 nitrogen atoms (N2 and N4) were identified from the difference Fourier synthesis map and constrained using AFIX commands. All other C-H-based hydrogen atoms were added using HFIX/AFIX commands. Crystal data, data collection parameters and refinement statistics are listed in Table S1. These data can be obtained free of charge via www.ccdc.cam.ac.uk/conts/retrieving.html or from the Cambridge Crystallographic Data Center, 12, Union Road, Cambridge CB2 1EZ; fax:(+44) 1223-336-033; or deposit@ccdc.cam.ac.uk. CCDC reference number 818011.

Table S1: Summary of the crystallographic information

	Compound **3**
Formula	$C_{94}H_{138}Mo_8N_{16}O_{31}Ru_2S_5$
M_r g mol^{-1}	3118.17
crystal system	Triclinic
space group	*P*-1
a [Å]	12.2930(12)
b [Å]	16.142(7)
c [Å]	17.387(4)
α [°]	92.43(3)
β [°]	95.969(9)
γ [°]	99.74(2)
V [Å^3]	3375.7(17)

ρ_{cald} [g cm^{-3}]	1.541
Z	1
$\mu(Mo_{K\alpha})$ mm^{-1}	1.079
T [K]	150(2)
no. rflns (measd)	81121
no. rflns (unique)	13766
no. params	751
*R*1 (I>2σ(I)	0.0492
*wR*2 (all data)	0.1571
GooF	1.090
Largest diff peak / hole	1.84 / -0.94

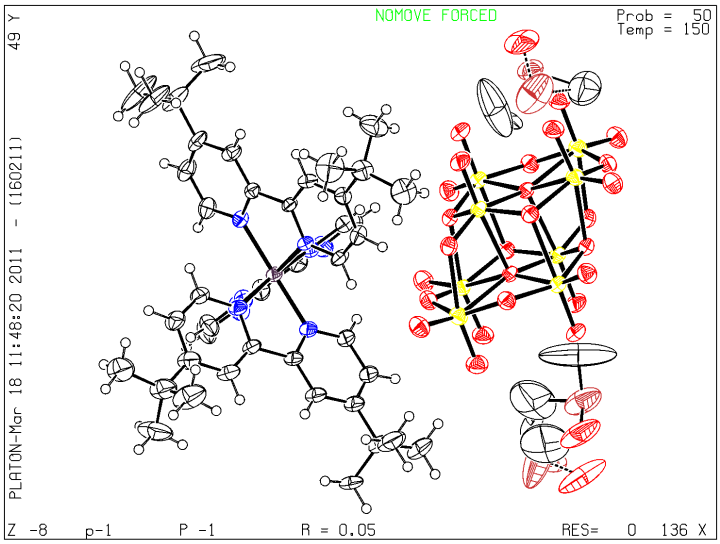

Figure S 1: ORTEP-plot of compound **3**, probability ellipsoids given at 50 %. The anisotropic displacement parameters of the DMSO solvent molecules are enlarged due to solvent disorder. All non-hydrogen atoms were refined anisotropically. The disordered C46, C47 and C48 atoms (based on DMSO solvent molecules) are ISOR restrained.

4. ^{1}H-NMR-titration experiments

NMR titration experiments were performed as follows: for each measurement, compound **1** and compound **2** were weighed out according to the molar ratios required and were dissolved in a given volume of DMSO-d6. The **1**:**2** molar ratios measured were 8:1, 4:1, 2:1, 1:1, 1:2, 1:4 and 1:8.

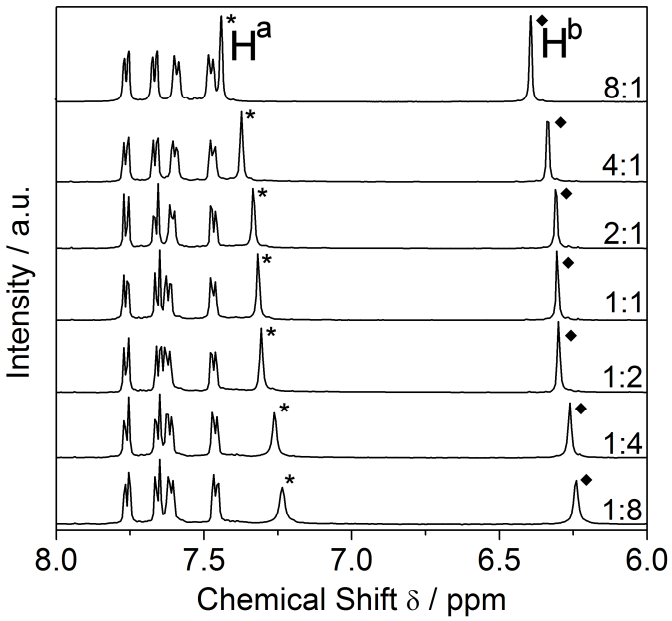

Figure S 2: ^{1}H-NMR spectroscopic monitoring of the changes of the chemical shifts of the biH$_2$-based protons H^a (*) and H^b (♦) depending on the **1**:**2** molar ratios (1:8 → 8:1).

5. UV-Vis and emission spectroscopic titration

UV-Vis and emission spectroscopic titrations at various **1**:**2** molar ratios were performed as follows: a 0.35 mM solution of compound **1** in DMSO and a 1.4 mM solution of compound **2** in DMSO were prepared. A set volume of compound **1** (1.0 ml) was mixed with the corresponding volume of compound **2** according to the **1**:**2** molar ratio required and the sample volume was made up to 3.0 ml so as to maintain a constant concentration of the luminescent compound **1**. The solutions were subsequently measured using UV-Vis and emission spectroscopy (excitation wavelength: 497 nm).

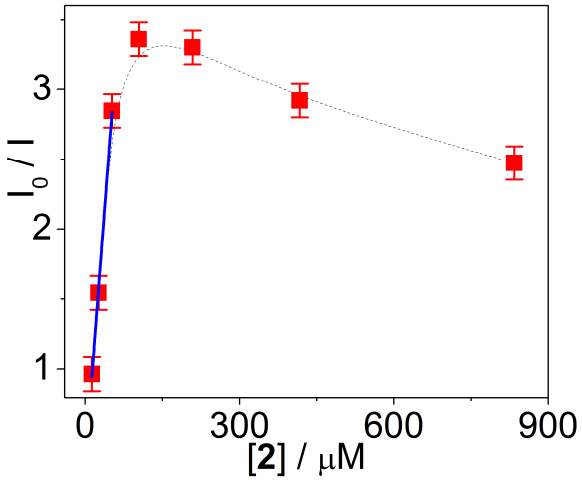

Figure S 3: Stern-Volmer-Plot at concentrations of [**1**] = 115 μM. The linear fit allowed the calculation of the Stern-Volmer constant k_{SV} = 48395 (± 1390) M^{-1}.

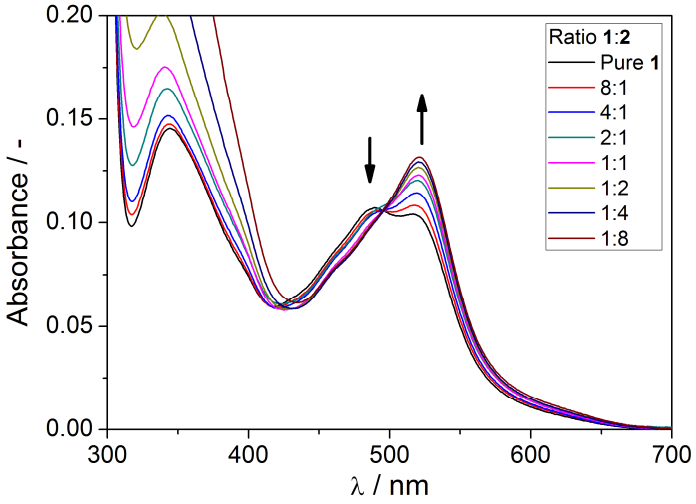

Figure S 4: UV-Vis titration at **1**:**2** ratios of 8:1 to 1:1 and concentration of [**1**] = 11 µM.

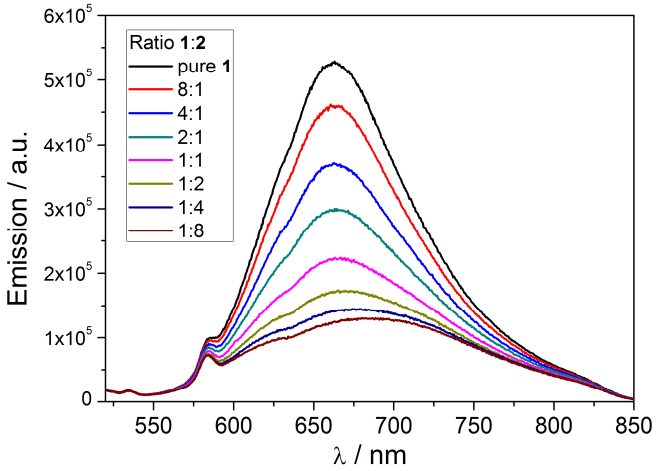

Figure S 5: Emission spectroscopic titration at **1**:**2** ratios of 8:1 to 1:8 and a concentration of [**1**] = 11 µM.

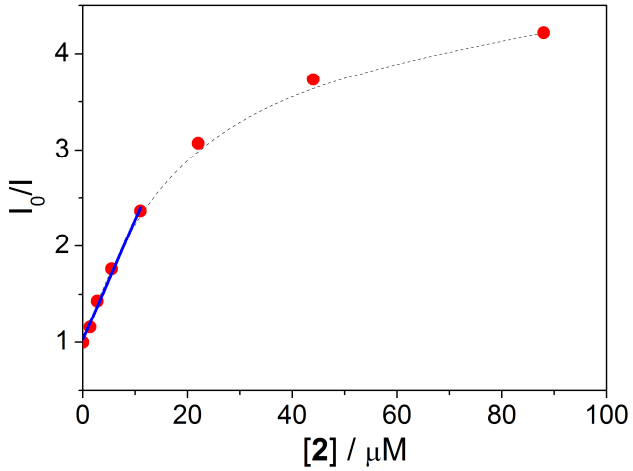

Figure S 6: Stern-Volmer-Plot at concentration of [**1**] = 11.0 µM. The linear fit allowed the calculation of the Stern-Volmer constant k_{SV} = 124330 (± 6550) M^{-1}. The effect of the increasing TBA concentration ([TBA] increases linearly with [**2**]) is still observable, however, the effect is less pronounced as in the higher concentrated sample (see Fig. S3).

6. Electrospray ionization mass spectrometry (ESI-MS) measurements

ESI-MS measurements were performed on a mixture of **1** and **2** (molar ratio 1:1, concentration: approx. 1x 10^{-4} M in acetonitrile) to see whether any {**1**·**2**} aggregates can be observed by mass-spectrometry. Data analysis showed that in negative ion mode, a prominent peak at m/z = 977.73 can be assigned to a 1:1 aggregate of **1** and **2** of the type $\{[Ru(tbbpy)_2(biH_2)][Mo_8O_{26}]\}^{2-}$. The observed difference in isotopic pattern is due to the effect of a second peak at lower m/z values which partially overlaps with the observed signal.

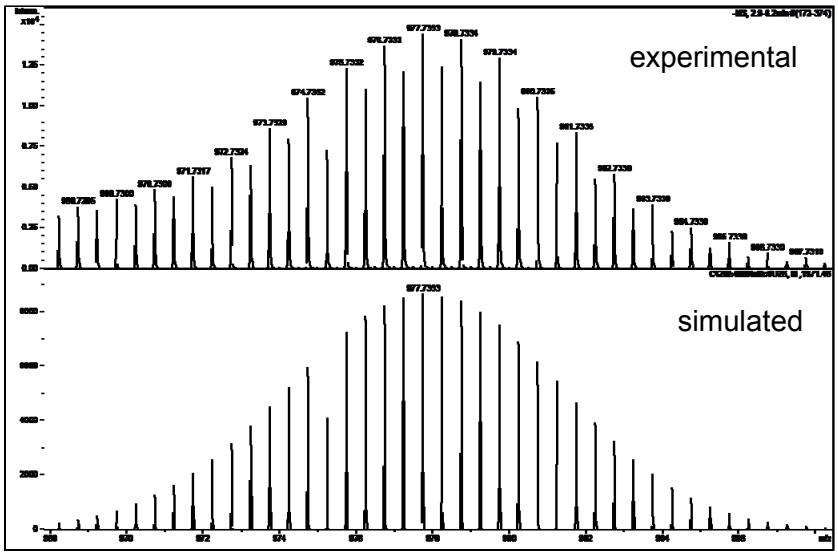

Figure S 7: ESI-MS analysis showing the experimentally observed peak for $\{[Ru(tbbpy)_2(biH_2)][Mo_8O_{26}]\}^{2-}$ at m/z = 977.73 (top) and the simulated pattern (bottom).

7. De-aggregation experiments by addition of TBABr

7.1. ^{1}H-NMR spectroscopy

To investigate the effect of an increased concentration of TBABr on the **1**:**2** interactions observed by ^{1}H-NMR-spectroscopy, an aliquot of TBABr was added to a mixture of **1** and **2** (molar ratio: 1:1) in DMSO-d6. The results show that after addition of TBABr, the two marker signals H^a and H^b show upfield shifts characteristic of a decreased interaction of **1** and **2** at the hydrogen-bonding site of the biH_2-ligand in **1**. This is interpreted as a de-aggregation of the {**1**·**2**} aggregates caused by the competitive formation of {TBA·**2**} ion pairs.

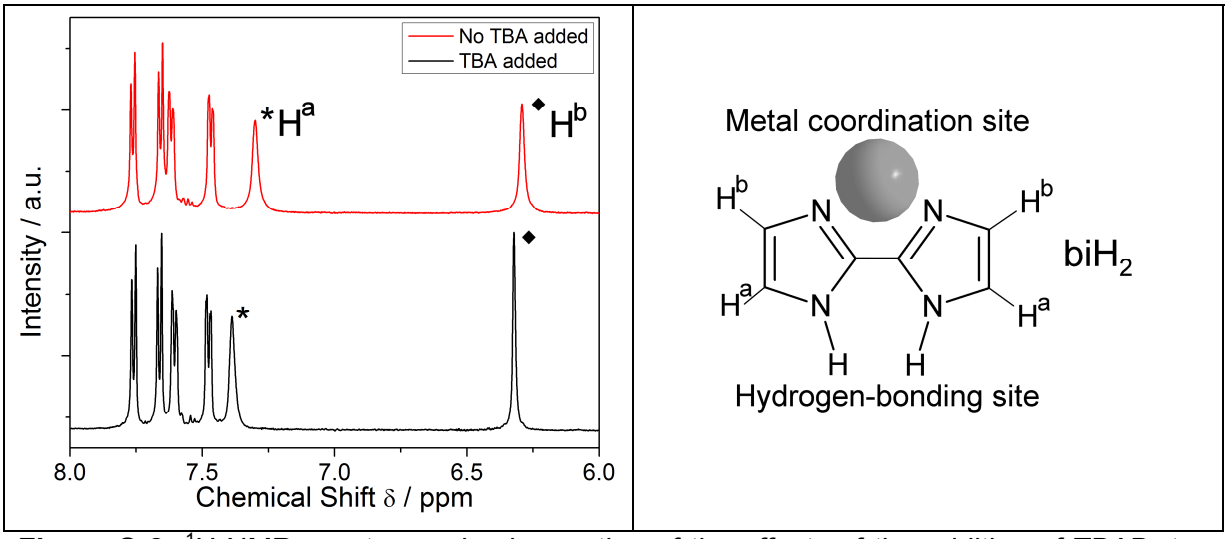

Figure S 8: ^{1}H-NMR-spectroscopic observation of the effects of the addition of TBABr to a 1:1 solution of **1** and **2** in DMSO-d6. Upon addition of an aliquot of TBABr, the marker protons H^a and H^b show an upfield shift, indicating the de-aggregation of the {**1**·**2**} aggregates in solution by the formation of {TBA·**2**} ion pairs.

6.2. Emission spectroscopy

To investigate the effect of an increased concentration of TBABr on the luminescence **1**, an aliquot of TBABr was added to a mixture of **1** and **2** (molar ratio: 1:1) in DMSO. The resulting emission spectrum shows a higher emission intensity which suggests that the quenching mechanism has been effectively disrupted. This suggests that the {**1**·**2**} aggregates are de-aggregated by the formation of {TBA·**2**} ion pairs.

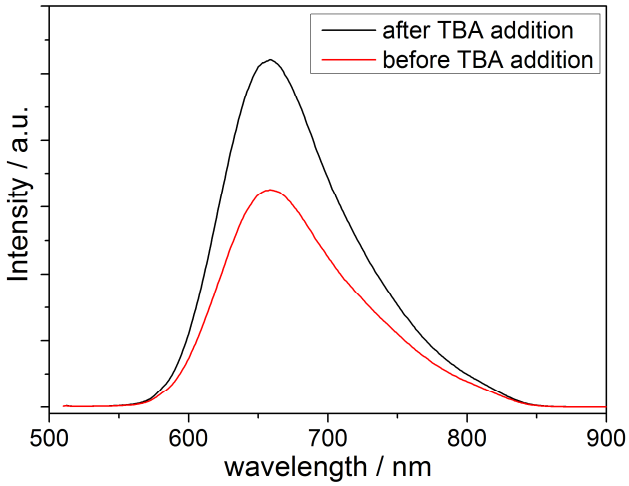

Figure S 9: Emission spectroscopy (excitation wavelength: 497 nm) of a mixture of **1** and **2** (molar ratio: 1:1, in DMSO) before and after the addition of an aliquot of TBABr. The graph illustrates that the emission intensity is increased, suggesting that the quenching mechanism is disrupted. This is interpreted as a de-aggregation of the {**1**·**2**} aggregates by competitive formation of {TBA·**2**} ion pairs.

7. Literature references cited in Electronic Supporting Information

S1 N. Rockstroh, K. Peuntinger, H. Görls, D. M. Guldi, F. W. Heinemann, B. Schäfer and S. Rau, *Z. Naturforsch.* 2010, **65b**, 281.

S2 M. McCann, K. Maddock, C. Cardin, M. Convery and G. Ferguson, *Polyhedron* 1995, **14**, 3655.

S3 G. M. Sheldrick, *Acta Crystallogr.* 2008, **A64**, 112.

S4 L. J. Farrugia, *J. Appl. Cryst.* 1999, **32**, 837.

S5 R. H. Blessing, *Acta Crystallogr.* 1995, **A51**, 33.

S6 P. Coppens, L. Leiserowitz and D. Rabinovich, *Acta Crystallogr.* 1965, **18**, 1035.

S7 A. L. Spek, *Acta Crystallogr.* 2009, **D65**, 148.